Journal of Dental Research
2021, Vol. 100(4) 377–386

DOI: 10.1177/0022034520965141
journals.sagepub.com/home/jdr

mTOR Inhibition Ablates Cisplatin-Resistant Salivary Gland Cancer Stem Cells

T. Nakano[1,2], K.A. Warner[1], A.E. Oklejas[1], Z. Zhang[1], C. Rodriguez-Ramirez[1], A.G. Shuman[3], and J.E. Nör[1,3,4,5]

Abstract

Patients with advanced salivary gland mucoepidermoid carcinoma (MEC) are treated with surgery and radiotherapy, as current systemic therapies are largely ineffective. As such, current treatment frequently leads to poor long-term survival due to locoregional recurrence or metastases. We have shown that salivary gland cancer stem cells (CSCs) are resistant to platinum-based chemotherapy and drive tumor progression. The purpose of this study was to investigate the effect of therapeutic inhibition of mTOR (mechanistic target of rapamycin) on resistance of CSCs to cisplatin, a prototypic platinum-based chemotherapeutic agent. Viability assays determined the effect of several inhibitors of PI3k/mTOR signaling (e.g., temsirolimus, BKM120, AZD8055, PF4708671) and/or cisplatin on survival of human MEC cells. The impact of mTOR inhibitors and/or cisplatin on MEC stemness was examined with salisphere assays, flow cytometry for ALDH/CD44 (CSC markers for MEC), and Western blots for Bmi-1 expression (marker of stem cell self-renewal). Salivary gland MEC patient-derived xenografts were used to examine the effect of cisplatin and/or temsirolimus on CSCs in vivo. We observed that cisplatin induced mTOR and S6K1 phosphorylation, increased the number and size of MEC salispheres, and induced Bmi-1 expression and the fraction of CSCs in MEC models in vitro. Cisplatin also increased the fraction of CSCs in vivo. In contrast, mTOR inhibition (e.g., temsirolimus) blocked cisplatin-induced Bmi-1 expression and salisphere formation in vitro. Remarkably, temsirolimus slowed down tumor growth and decreased the fraction of CSCs ($P < 0.05$) even in presence of cisplatin in a short-term in vivo experiment. Collectively, these results demonstrate that therapeutic inhibition of mTOR ablates cytotoxic-resistant CSCs, and they suggest that a combination of an mTOR inhibitor and platinum-based chemotherapy might be beneficial to patients with salivary gland mucoepidermoid carcinoma.

Keywords: tumor initiating cell, self-renewal, rapamycin, chemotherapy, targeted therapy, head and neck cancer

Introduction

Mucoepidermoid carcinoma (MEC) corresponds to about 30% of all salivary gland malignancies (Luna 2006) and is classified into 3 grades (low, intermediate, high) depending on histologic findings. The effectiveness of standard of care (surgery + chemoradiotherapy) is modest in patients with high-grade MEC. Indeed, advanced/recurrent disease engenders significant morbidity and mortality (Laurie and Licitra 2006; Chen et al. 2007; Vander Poorten et al. 2014; Alfieri et al. 2017). As such, the development of a mechanism-based, effective, and safe systemic therapy for patients with MEC is urgently needed.

Cancer stem cells (CSCs) constitute a subpopulation of unique tumor cells that exhibit a stem-like state and were shown to drive tumor relapse and metastasis (Al-Hajj et al. 2003; Hambardzumyan et al. 2006; Ailles and Weissman 2007; Carmalt et al. 2009; Charafe-Jauffret et al. 2010; Zhang et al. 2012; Adams et al. 2013; Fitzgerald and McCubrey 2014; Kim et al. 2017). Interestingly, platinum-based chemotherapy induces self-renewal and increases the CSC fraction in several cancer types, including head and neck squamous cell carcinoma (HNSCC; Chen et al. 2012; Korkaya et al. 2012; Nör et al. 2014). We recently demonstrated that salivary gland MEC follows the CSC hypothesis and that high aldehyde dehydrogenase (ALDH) activity and CD44 expression identify CSCs as uniquely tumorigenic cells in MEC (Adams et al. 2015). While no marker combination can pick up all cells exhibiting a CSC state, the ALDH/CD44 combination exhibited the highest sensitivity and specificity among the markers evaluated. Nevertheless, work demonstrating that MDM2-p53 inhibitors target MEC CSCs (Andrews et al. 2019) contributed

[1]Department of Cariology, Restorative Sciences, and Endodontics, School of Dentistry, University of Michigan, Ann Arbor, MI, USA
[2]Department of Otorhinolaryngology, Graduate School of Medical Sciences, Kyushu University, Fukuoka, Japan
[3]Department of Otolaryngology–Head and Neck Surgery, School of Medicine, University of Michigan, Ann Arbor, MI, USA
[4]Department of Biomedical Engineering, College of Engineering, University of Michigan, Ann Arbor, MI, USA
[5]Rogel Cancer Center, University of Michigan, Ann Arbor, MI, USA

A supplemental appendix to this article is available online.

Corresponding Author:
J.E. Nör, University of Michigan, 1011 N. University, Rm. G049, Ann Arbor, MI 48109-1078, USA.
Email: jenor@umich.edu

to the recent approval of a clinical trial testing APG-115 in salivary gland malignancies (NCT03781986).

The mechanistic target of rapamycin (mTOR) is one of the important downstream protein kinases of the PI3K/AKT signaling pathway. It forms 2 distinct complexes: mTOR complex 1 (mTORC1) and mTOR complex 2 (mTORC2). mTORC1 contains Raptor (regulatory-associated protein of mTOR), a downstream target of AKT that regulates the ribosomal S6 protein kinase 1 (S6K1) and eukaryotic translation initiation factor 4E-binding protein 1 and mediates cell proliferation and protein synthesis (Saxton and Sabatini 2017). However, mTORC2 contains Rictor (rapamycin insensitive companion of mTOR), which controls the activation of AKT and plays key roles in cell proliferation, survival, and metabolism (Saxton and Sabatini 2017). Several studies have shown that the activation of mTOR signaling is associated with poor prognosis in patients with malignant tumors (Ocana et al. 2014). Indeed, mTOR inhibitors such as rapamycin and rapamycin analogs (e.g., temsirolimus, everolimus) have been approved for renal cell carcinoma. In addition, ongoing clinical trials are using this class of drugs in other carcinomas, including HNSCC (Janku et al. 2018; Magaway et al. 2019). Notably, studies with PI3K inhibitors that have an impact on mTOR signaling have shown effects on CSCs (Hu et al. 2015; Keysar et al. 2016; Trucco et al. 2018; Zhou et al. 2019). Considering our recent observation that MEC CSCs exhibit constitutive activation of the mTOR pathway (Adams et al. 2015), we decided to evaluate the impact of therapeutic inhibition of mTOR in preclinical models of salivary MEC.

Conventional chemotherapy induces stemness in tumors such as HNSCC, glioblastoma, and breast cancer (Chen et al. 2012; Korkaya et al. 2012; Nör et al. 2014). However, the effect of mTOR inhibitors on cisplatin-induced MEC CSCs is unclear. We observed that cisplatin causes an increase in the fraction of CSCs and that therapeutic inhibition of mTOR ablates cisplatin-induced stemness in preclinical models of MEC.

Materials and Methods

Detailed description of the methods employed in this study can be found in the Appendix (i.e., SRB assay, salisphere assay, flow cytometry, Western blots, patient-derived xenograft model of MEC, and histologic and statistical analyses).

Results

Cisplatin Enhances Self-renewal (Bmi-1) and MEC Stemness

To evaluate the effect of a platinum-based chemotherapeutic agent on bulk MEC cell viability, human MEC cells (UM-HMC-1, UM-HMC-3A, UM-HMC-3B) verified by short-tandem repeat profiling (Appendix Fig. 1) were treated with increasing concentrations of cisplatin for 24 to 72 h. The half maximal inhibitory concentration (IC_{50}) for cisplatin ranged from 0.62 to 6.34 μM (48 h) and from 0.06 to 0.24 μM (72 h), but treatment for 24 h did not reach IC_{50} (Appendix Fig. 2). As expected, the UM-HMC-3B cell line generated from metastasis (same patient as the UM-HMC-3A cells) was the most resistant, as we have observed when testing other drugs (Andrews et al. 2019). To investigate the effect of cisplatin on the fraction of CSCs in vitro, we performed flow cytometry in MEC cells (Fig. 1A). We observed an increase in the fraction of $ALDH^{high}CD44^{high}$ cells upon treatment with cisplatin in 3 MEC cell lines (Fig. 1B). In addition, cisplatin increased the number and size of MEC salispheres in ultralow attachment plates (Fig. 1C–E) and induced expression of Bmi-1, a major activator of stem cell self-renewal (Fig. 2A). Notably, cisplatin induced phosphorylation of mTOR and S6K1 (downstream target of mTOR signaling) and expression of Raptor but did not mediate consistent changes in the expression of Rictor and pAKT. Collectively, these results indicate that cisplatin activates the mTORC1 complex (Saxton and Sabatini 2017) and induces MEC stemness in vitro.

Temsirolimus Inhibits Bmi-1 Expression and MEC Stemness

To examine the impact of different types of the PI3K/mTOR pathway inhibitors on the viability of MEC cells, we treated UM-HMC cell lines with increasing concentrations of a PI3K inhibitor (buparlisib), 2 mTOR inhibitors (temsirolimus and AZD8055), or an S6K1 inhibitor (PF4708671). All inhibitors exhibited a dose- and time-dependent effect on cell viability in MEC cell lines (Appendix Fig. 3). Then, we treated UM-HMC cells with one of the mTOR inhibitors and cisplatin for 24 to 72 h. The combination of temsirolimus and cisplatin was the most effective in UM-HMC-1 and UM-HMC-3A cells, whereas the combination of AZD8055 and cisplatin was the most effective in the UM-HMC-3B cell line at 72 h (Fig. 2B). Considering that temsirolimus is a clinically relevant drug in the context of oncology (Food and Drug Administration approved for renal cell carcinoma), we decided to focus the remaining of this project on combination therapies involving this drug. The combination index–isobologram method showed that 1 μM cisplatin displays a synergistic effect when combined with ≥0.001 μM temsirolimus or when combined with ≥0.1 μM temsirolimus on the viability of UM-HMC-1 and UM-HMC-3A cells, respectively (Appendix Fig. 4).

To begin to understand the impact of temsirolimus in MEC CSCs, we performed Western blots that confirmed inhibition of mTOR and S6K1 phosphorylation and inhibition of Bmi-1 in a dose-dependent manner, suggesting a possible effect of this drug on MEC self-renewal (Fig. 2C). Then, we assessed the effect of temsirolimus on the CSC fraction using flow cytometry for ALDH and CD44 (Fig. 3A). Temsirolimus caused a dose-dependent decrease in the fraction of $ALDH^{high}CD44^{high}$ cells in the 3 MEC cell lines evaluated, including the more resistant cell line (UM-HMC-3B; Fig. 3B). These data correlated with a decrease in the number of salispheres (Fig. 3C).

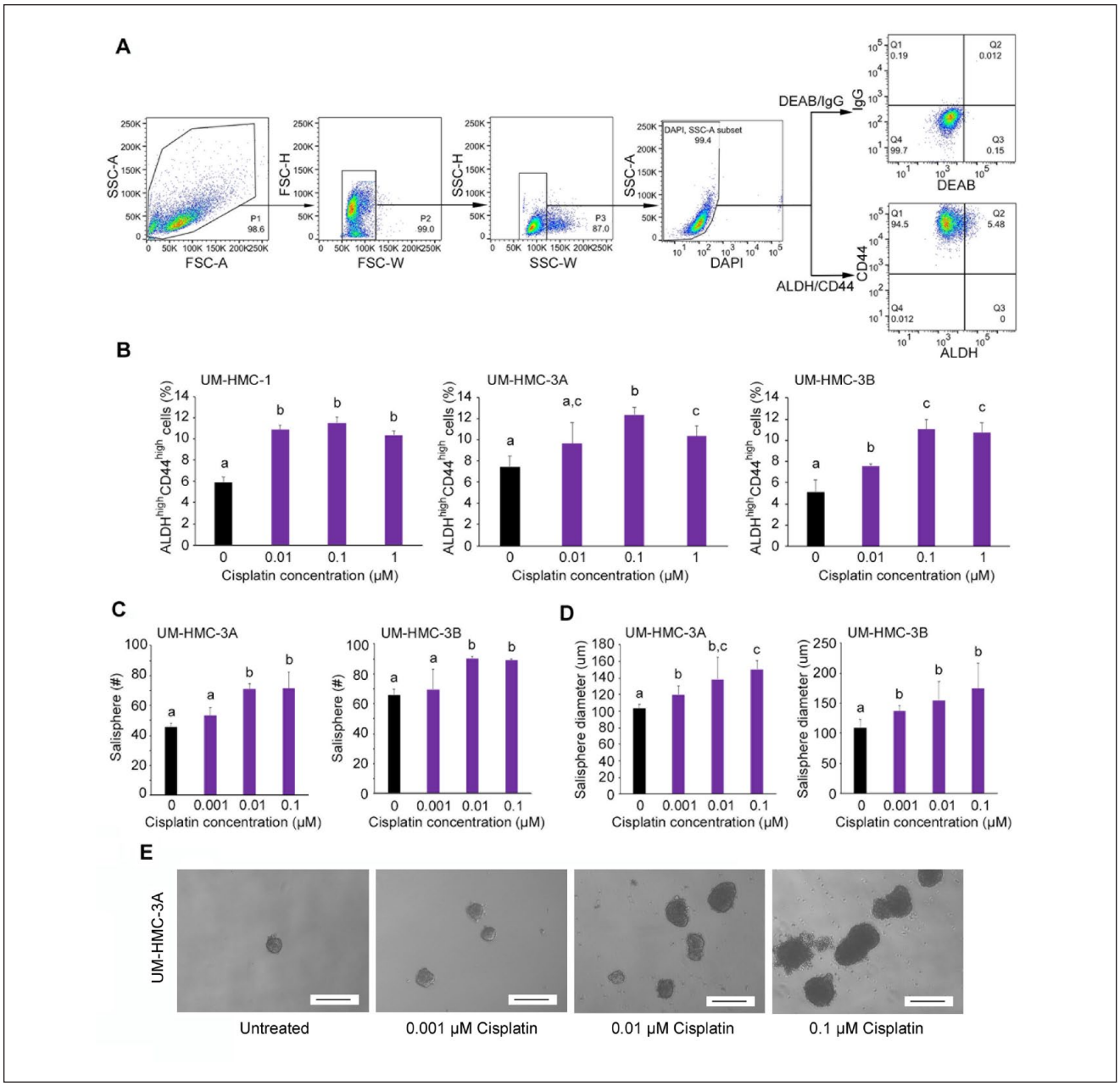

Figure 1. Cisplatin enhanced the fraction and size of cancer stem cells in vitro. (**A**) Example of flow cytometry gating strategy for cell lines. To identify cells of interest based on size and granularity, the initial analysis region used SSC-A versus FSC-A, FSC-H versus FSC-W, and SSC-H versus SSC-W. Viable cells were identified by SSC-A versus DAPI. The identification of $ALDH^{high}CD44^{high}$ cells was based on IgG versus DEAB control. A, area; FSC, forward scatter; H, height; SSC, side scatter; W, width. (**B**) Flow cytometry analysis of ALDH and CD44 staining status of UM-HMC-1, UM-HMC-3A, and UM-HMC-3B cells treated with serial dilution of cisplatin (0 to 1 μM) for 24 h. Bar graphs illustrate the percentage of mucoepidermoid carcinoma cancer stem cells (i.e., $ALDH^{high}CD44^{high}$ cells). (**C**, **D**) Bar graphs illustrate the average number and size of salispheres per well generated from UM-HMC-3A and UM-HMC-3B cell lines treated with cisplatin (0 to 0.1 μM). (**E**) Representative photographs of salispheres after treatment with cisplatin (0 to 0.1 μM). Scale bars represent 200 μm (×40). Values are presented as mean ± SD. Different lowercase letters represent statistical significance at $P < 0.05$ as determined by 1-way analysis of variance followed by post hoc tests. Experiments were performed in triplicate wells per condition, and graphs represent at least 3 independent experiments.

Surprisingly, the few salispheres that escaped treatment with temsirolimus grew to approximately the same size as those in the untreated control group (Fig. 3D). These data were corroborated with the small molecule inhibitor of Bmi-1 (PTC-209) that also caused a decrease in the number of salispheres ($P < 0.05$), even when combined with cisplatin (Appendix Fig. 5). Collectively, these data showed that temsirolimus inhibited the expression of Bmi-1 and reduced MEC stemness in vitro.

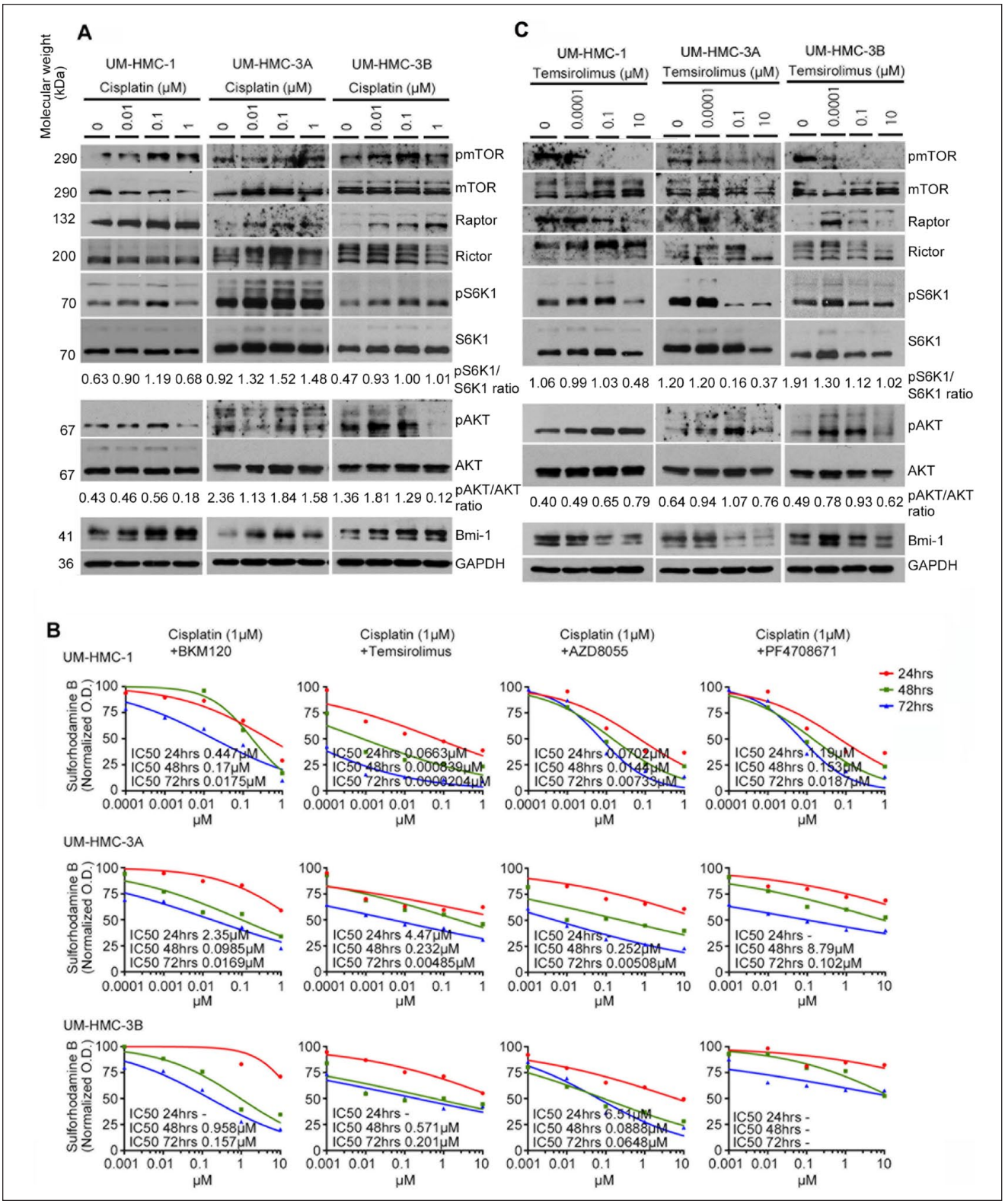

Figure 2. Effect of cisplatin or temsirolimus on expression of the mTOR signaling pathway, Bmi-1, and cell viability in vitro. (**A**) Western blot analysis of UM-HMC-1, UM-HMC-3A, and UM-HMC-3B cells treated with cisplatin (0 to 1 μM) for 24 h. (**B**) Combination of mTOR inhibitors with cisplatin was more effective than mTOR inhibitor alone in vitro. The cytotoxicity of combination therapy for 24, 48, and 72 h was evaluated by the SRB assay in UM-HMC-1, UM-HMC-3A, and UM-HMC-3B cell lines. Cisplatin was kept at fixed concentration (1 μM), while mTOR inhibitor was delivered at increasing concentrations. Data were normalized against vehicle control. Experiments were performed in triplicate wells per condition, and graphs represent at least 3 independent experiments. (**C**) Western blot analysis of UM-HMC-1, UM-HMC-3A, and UM-HMC-3B cells treated with temsirolimus (0 to 10 μM) for 24 h.

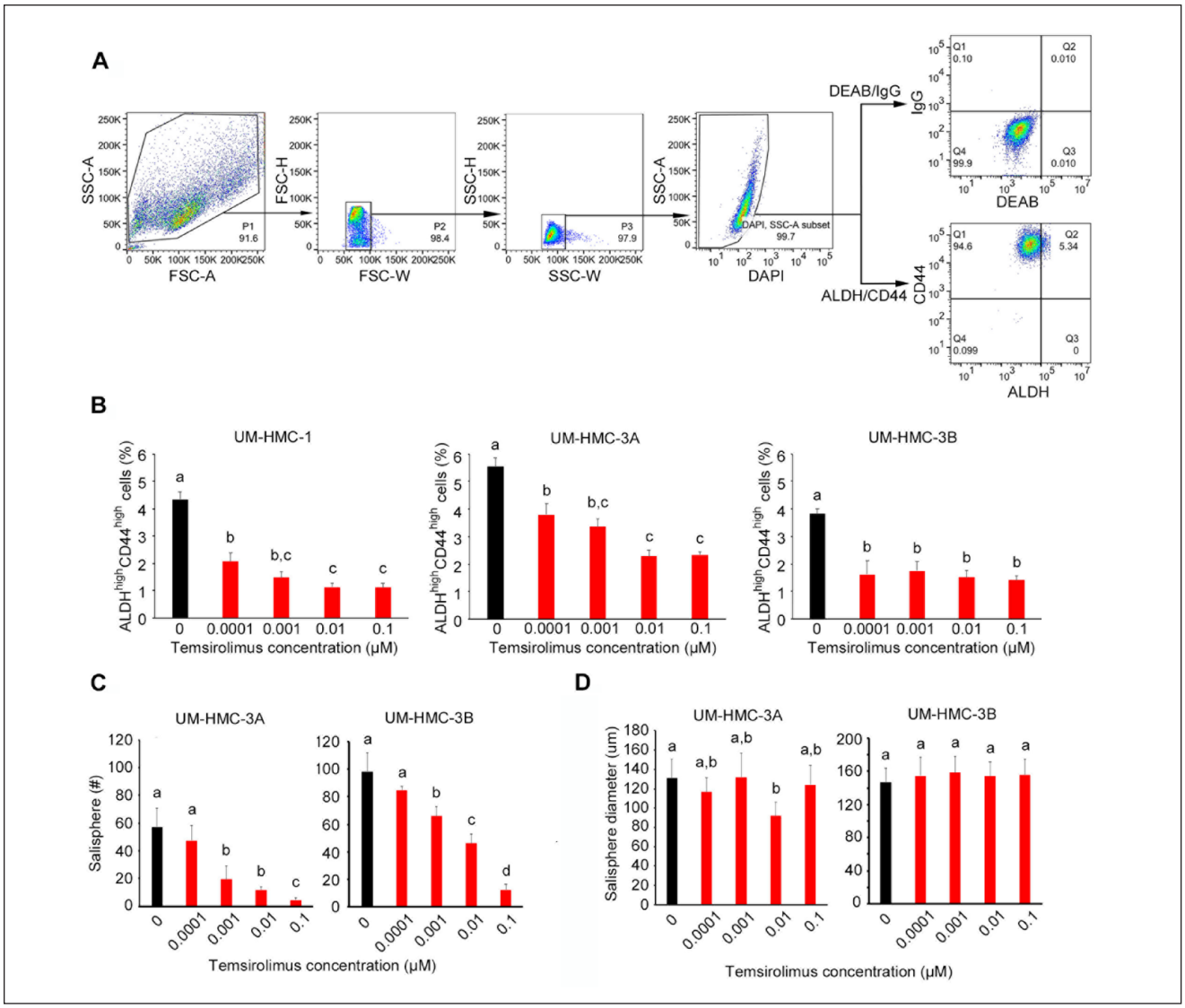

Figure 3. Effect of temsirolimus on cancer stem cells in vitro. (**A**) Example of flow cytometry gating strategy for cell lines. To identify cells of interest based on size and granularity, the initial analysis region used SCC-A versus FSC-A, FSC-H versus FSC-W, and SCC-H versus SCC-W. Alive cells were identified by SSC-A versus DAPI. The identification of $ALDH^{high}CD44^{high}$ cells was based on IgG versus DEAB control. A, area; FSC, forward scatter; H, height; SSC, side scatter; W, width. (**B**) Flow cytometry analysis of ALDH and CD44 staining status of UM-HMC-1, UM-HMC-3A, and UM-HMC-3B cells treated with a serial dilution of temsirolimus (0 to 0.1 μM) for 24 h. Bar graphs illustrate the percentage of $ALDH^{high}CD44^{high}$ cells. (**C**, **D**) Bar graphs illustrate the average number and size of salispheres per well generated from UM-HMC-3A and UM-HMC-3B cell lines treated with temsirolimus (0 to 0.1 μM). Values are presented as mean ± SD. Different lowercase letters represent statistical significance at $P < 0.05$ as determined by 1-way analysis of variance followed by post hoc tests. Experiments were performed in triplicate wells per condition, and graphs represent at least 3 independent experiments.

Temsirolimus Blocks Cisplatin-Induced Stemness of MEC Cells

To examine the effect of combination therapy and drug sequencing on CSCs, we treated MEC cells with temsirolimus and/or cisplatin and performed flow cytometry for ALDH and CD44 (Fig. 4A). Cisplatin alone consistently increased the CSC fraction, while temsirolimus alone decreased it (Fig. 4B). Temsirolimus was sufficient to block cisplatin-induced CSC fraction increase. Interestingly, when the impact of drug sequencing was evaluated, we observed that either temsirolimus first or temsirolimus and cisplatin together were more effective in reducing the fraction of CSCs than cisplatin first.

To further assess the effect of combination therapy on MEC stemness, salisphere assays were performed in ultralow attachment plates with temsirolimus and/or cisplatin for 8 d (Fig. 4C). Consistent with the CSC fraction data, cisplatin alone increased the number and size of salispheres when compared with untreated groups. In contrast, temsirolimus alone decreased the number of salispheres and had a modest effect in the sphere

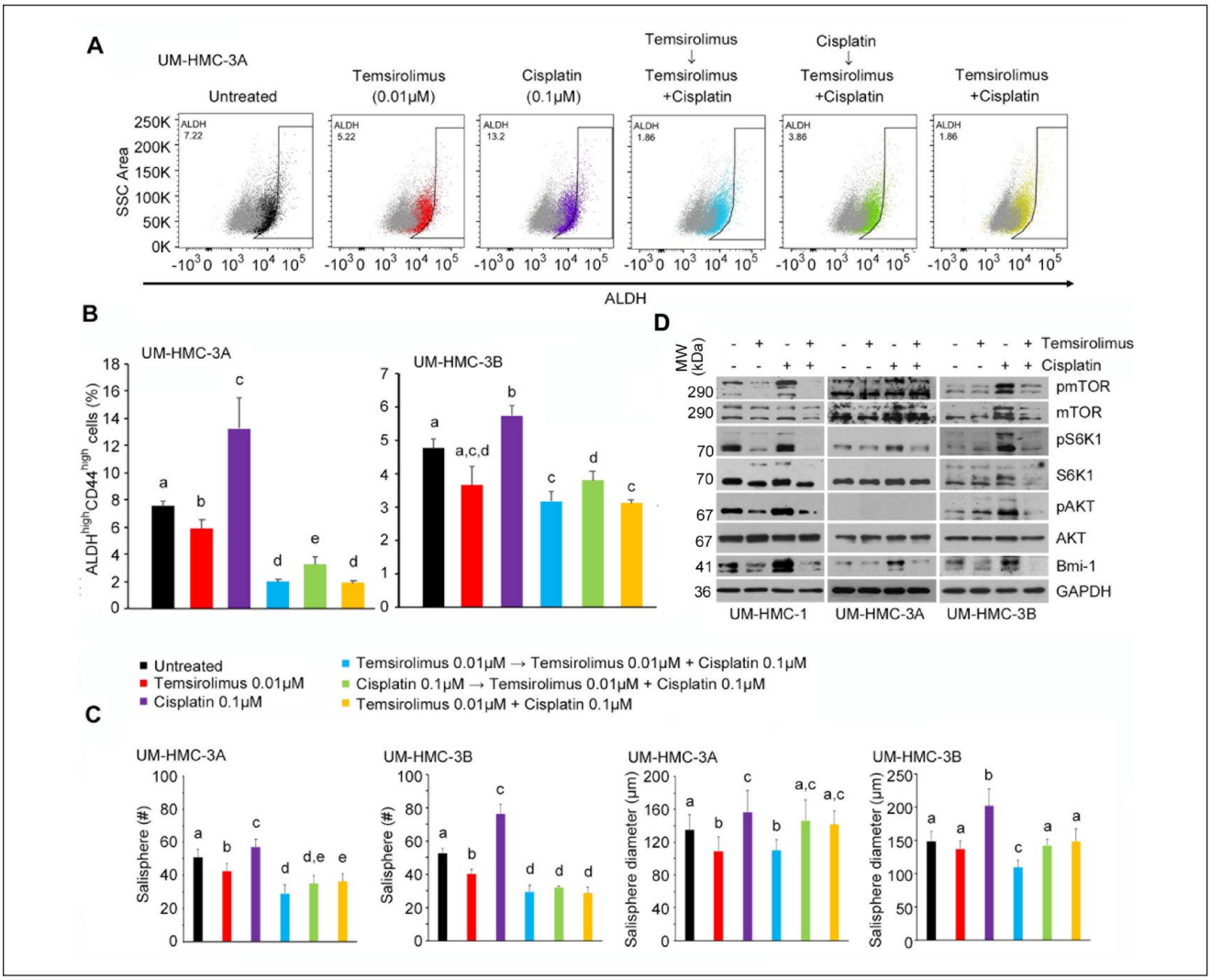

Figure 4. Effect of combination therapy on cancer stem cells in vitro. (**A**) Flow cytometry analysis of UM-HMC-3A cells stained for ALDH. The horizontal axis shows ALDH staining, while vertical axis shows side scatter (SSC) area. (**B**) Bar graphs illustrate the percentage of $ALDH^{high}CD44^{high}$ cells in UM-HMC-3A and UM-HMC-3B cell lines treated with temsirolimus (red, 0.01 μM); cisplatin (purple, 0.1 μM); temsirolimus (0.01 μM) first, then both temsirolimus (0.01 μM) and cisplatin (0.1 μM) 24 h later (light blue); cisplatin (0.1 μM) first, then both temsirolimus (0.01 μM) and cisplatin (0.1 μM) 24 h later (green); or temsirolimus (0.01 μM) and cisplatin (0.1 μM) at the same time (yellow). (**C**) Bar graphs illustrate the average number and size of salispheres per well generated from UM-HMC-3A and UM-HMC-3B cell lines treated with temsirolimus (red, 0.01 μM); cisplatin (purple, 0.01 μM); temsirolimus (0.01 μM) first, then both temsirolimus (0.01 μM) and cisplatin (0.01 μM) 24 h later (light blue); cisplatin (0.01 μM) first, then both temsirolimus (0.01 μM) and cisplatin (0.01 μM) 24 h later (green); or temsirolimus (0.01 μM) and cisplatin (0.01 μM) the at same time (yellow). (**D**) Western blot analysis of UM-HMC-1, UM-HMC-3A, and UM-HMC-3B cells treated with temsirolimus (0 or 0.1 μM) and cisplatin (0 or 0.1 μM) for 24 h. Values are presented as mean ± SD. Different lowercase letters represent statistical significance at $P < 0.05$ as determined by 1-way analysis of variance followed by post hoc tests. Experiments were performed in triplicate wells per condition, and graphs represent at least 3 independent experiments.

size. We also observed a consistent decrease in the number and size of spheres when combination therapy (particularly temsirolimus alone first, followed by treatment with temsirolimus and cisplatin together) was compared with cisplatin alone. To evaluate the effect of combination therapy in key mediators of stemness, we performed Western blots (Fig. 4D). By itself, cisplatin activated the mTOR pathway and induced Bmi-1 expression. However, when cisplatin was combined with temsirolimus, we observed a shutdown of the mTOR signaling pathway and an inhibition of Bmi-1 expression back to baseline levels.

Temsirolimus Abrogates Cisplatin-Mediated Increase in CSC Fraction In Vivo

To assess the effect of combination temsirolimus/cisplatin therapy in vivo, we generated patient-derived xenograft (PDX) MEC tumors and performed a short-term preclinical trial focused on the impact of therapy in stemness. When an average tumor size reached approximately 460 mm^3 (Appendix Fig. 6A), mice were randomly allocated into the 6 treatment regimens (Fig. 5A). All treatment regimens were well tolerated

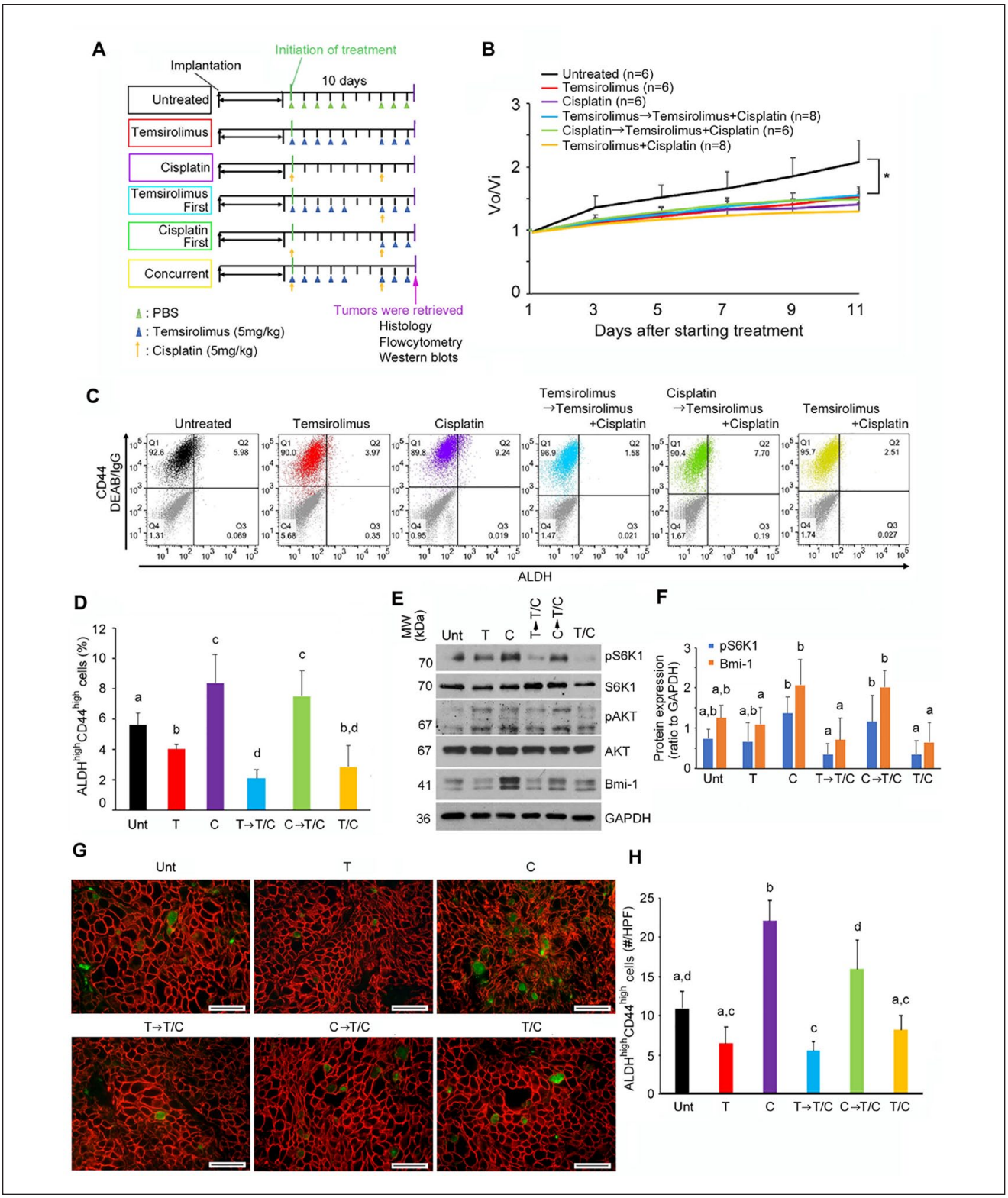

Figure 5. Effect of combination therapy on cancer stem cells in vivo. (**A**) Treatment schema. Mice harboring patient-derived xenograft (PDX) tumors were treated with phosphate-buffered saline (PBS) intraperitoneally (IP) daily (days 1 to 5 and 8 to 10), temsirolimus alone (5 mg/kg/d, IP, days 1 to 5 and 8 to 10), cisplatin alone (5 mg/kg/d, IP, days 1 and 8), temsirolimus-first combination therapy (temsirolimus, 5 mg/kg/d, IP, days 1 to 5 and 8 to 10; cisplatin, 5 mg/kg, IP, day 8), cisplatin-first combination therapy (cisplatin, 5 mg/kg/d, IP, days 1 and 8; temsirolimus, 5 mg/kg/d, IP, days 8 to 10), and

by mice (Appendix Fig. 6B) and caused a modest (but significant) inhibition of tumor growth as compared with the untreated group (Fig. 5B). Histologically, PDX tumors showed similar morphology as the primary human tumor, being composed of intermediate and squamoid cells exhibiting mitosis, anaplasia, some areas of necrosis, and mucinous cell-like differentiation (Appendix Fig. 7). Immunohistochemical analyses showed that PDX tumors were positive for pan-cytokeratin, and biochemical staining showed PAS-positive cells scattered throughout the PDX tumors.

We performed flow cytometry to evaluate the effect of treatment on CSC fraction (Fig. 5C). Consistent with in vitro results, cisplatin alone resulted in an increase in the CSC fraction in MEC PDX tumors (Fig. 5D). In contrast, temsirolimus alone mediated a decrease in the CSC fraction. Combination therapy showed interesting results. When we started treatment with cisplatin alone, followed by combination treatment with temsirolimus and cisplatin, the CSC fraction remained higher than untreated controls (at levels that were similar to cisplatin alone). However, when we used cisplatin and temsirolimus together or started with temsirolimus alone followed by combination therapy, the fraction of CSCs was remarkably decreased. Collectively, these data showed that while treatment sequence has no major influence on short-term tumor volume, it does have a major impact on the fraction of CSCs in vivo.

Western blots of PDX tumor lysates (Fig. 5E, F) showed strong correlation with flow cytometry data (Fig. 5D). Cisplatin alone caused phosphorylation of S6K1 and potent induction of Bmi-1. A similar trend is observed when we did combination therapy starting with cisplatin. In contrast, combination therapies starting with temsirolimus alone or both drugs showed inhibition of S6K1 phosphorylation and ablation of cisplatin-induced Bmi-1 upregulation. The Akt signaling pathway promotes anti-inflammatory responses in macrophages (Vergadi et al. 2017). To evaluate the effect of mTOR inhibition combined (or not) with cisplatin on tumor-associated macrophages, we performed immunohistochemistry for F4/80 in PDX tumors treated with temsirolimus and/or cisplatin (Appendix Fig. 8). We observed that cisplatin is associated with a nonsignificant trend for an increase in the number of tumor macrophages, as compared with untreated controls. However, temsirolimus caused a decrease in the number of macrophages when compared with cisplatin-treated tumors ($P < 0.05$).

To verify the results obtained with flow cytometry, we performed immunofluorescence staining for ALDH1 and CD44 in the MEC PDX tumors. While most tumor cells exhibited cell membrane CD44 staining, only a few cells dispersed throughout the tissue showed ALDH1 staining (Appendix Fig. 9). The results of these histologic analyses (Fig. 5G, H) confirmed the same trends showed by flow cytometry (Fig. 5D). 1) Cisplatin alone increased the CSC fraction; 2) temsirolimus alone, temsirolimus first followed by combination temsirolimus/cisplatin, or combination temsirolimus/cisplatin therapy throughout experimental period reduced the CSC fraction; and 3) treatment with cisplatin first followed by combination therapy was not effective at reducing CSC fraction (Fig. 5H).

Discussion

Resistance to systemic therapy is a major challenge in the management of patients with advanced salivary gland MEC. As such, today's treatment for these patients remains largely focused on surgery. However, a considerable number of patients experience disease progression, exhibiting locoregional recurrence and distant metastases. Knowing that CSCs mediate therapeutic resistance and drive cancer progression in many tumor types (Chen et al. 2012; Korkaya et al. 2012; Chinn et al. 2015), we performed here a series of studies attempting to find a therapeutic strategy to ablate CSCs in MEC.

Cisplatin is the first-line cytotoxic agent for patients with advanced head and neck carcinoma, including salivary gland MEC. However, cisplatin alone is not an adequate or effective treatment of advanced MEC (Laurie and Licitra 2006; Chen et al. 2007; Vander et al. 2014; Alfieri et al. 2017). Considering that the CSCs may drive resistance to platinum-based agents, we looked for possible vulnerabilities in these cells and observed that MEC CSCs exhibit a constitutively active mTOR pathway (Adams et al. 2015). Here, we evaluated 4 types of inhibitors of the PI3K-mTOR signaling pathway for possible effects on CSCs. Although we observed varying effectiveness for each inhibitor in different cell lines, the combination of mTOR inhibitor and cisplatin was consistently more effective

concurrent therapy (temsirolimus, 5 mg/kg/d, IP, days 1 to 5 and 8 to 10; cisplatin, 5 mg/kg, IP, days 1 and 8). (**B**) Line graph illustrates the observed tumor volume (Vo) normalized against initial tumor volume (Vi) immediately before treatment was initiated. UM-HMC-PDX-18 tumor treated with PBS (untreated, $n = 6$, black), temsirolimus ($n = 6$, red), cisplatin ($n = 6$, purple), temsirolimus-first combination therapy ($n = 8$, light blue), cisplatin-first combination therapy ($n = 6$, green), or temsirolimus and cisplatin at the same time ($n = 8$, yellow). (**C**) Flow cytometry analysis of UM-HMC-PDX-18 stained for ALDH and CD44. The horizontal axis shows ALDH staining, while the vertical axis shows CD44. (**D**) Bar graphs illustrate the percentage of $ALDH^{high}CD44^{high}$ cells in UM-HMC-PDX-18 treated with PBS (untreated [Unt], $n = 6$, black), temsirolimus (T; $n = 6$, red), cisplatin (C; $n = 6$, purple), temsirolimus-first combination therapy (T→T/C; $n = 8$, light blue), cisplatin-first combination therapy (C→T/C; $n = 6$, green), or temsirolimus and cisplatin at the same time (T/C; $n = 8$, yellow). (**E**, **F**) Western blot analysis of representative UM-HMC-PDX-18 tumor tissue lysates from each treatment group: Unt, T, C, T→T/C, C→T/C, and T/C. Bar graphs illustrate the quantification of pS6K1 and Bmi-1 normalized against GAPDH. Band densities were quantified with ImageJ software (National Institutes of Health). (**G**) Images show representative photographs of immunofluorescence staining of UM-HMC-PDX-18 tumor tissue sections stained for ALDH1 (green) and CD44 (red). Images were taken at 400× magnification, and scale bars represent 50 µm. (**H**) Bar graph illustrates the number of positive cells for ALDH1 and CD44 per high-power field (HPF; 400× magnification) in tissues from UM-HMC-PDX-18 mice treated with temsirolimus (red), cisplatin (purple), temsirolimus-first combination therapy (light blue), cisplatin-first combination therapy (green), or temsirolimus and cisplatin at the same time (yellow). Values are presented as mean ± SD. Different lowercase letters represent statistical significance at $P < 0.05$ as determined by 1-way analysis of variance followed by post hoc tests.

than the targeted drug alone or cisplatin alone. Given that combination therapies involving temsirolimus were the most effective in 2 of the 3 MEC cell lines evaluated and that it is Food and Drug Administration approved for another carcinoma (i.e., advanced renal cell carcinoma), we decided to focus the majority of our studies on combination therapy involving temsirolimus and cisplatin.

Key findings of this study are as follows. 1) Platinum-based chemotherapy with cisplatin induces Bmi-1 expression and increases the CSC fraction in MEC in vivo. The increase in CSC fraction is attributed to the resistance of CSCs to cisplatin and compounded by the induction of Bmi-1 and consequent increase in stem cell self-renewal mediated by this drug. 2) Targeted inhibition of mTOR signaling with temsirolimus blocks expression of cisplatin-induced Bmi-1 and increase in the CSC fraction in vivo. These results suggest a possible mechanism for the high frequency of tumor relapse when patients with MEC are treated with cisplatin; that is, this drug is not only ineffective at eliminating CSCs but actually induces the self-renewal and accumulation of CSCs that are considers "drivers" of tumor progression (Chen et al. 2012; Korkaya et al. 2012; Chinn et al. 2015). These data also suggest a possible strategy to overcome the negative effect of cisplatin in MEC—specifically, to combine it with an inhibitor of mTOR signaling, as MEC CSCs are apparently "addicted" to this pathway.

Multiple signaling pathways regulate Bmi-1 expression in cancer, including the Akt, TWIST1, and c-Myc pathways (Nacerddine et al. 2012; Liu et al. 2019). As such, it was rather surprising that inhibition of mTOR/Akt signaling with temsirolimus was sufficient to mediate dose-dependent inhibition of Bmi-1 expression and abrogate cisplatin-induced upregulation of Bmi-1 in the 3 MEC cell lines evaluated here. One concludes that while there are many upstream regulators of Bmi-1 expression, the Akt pathway is somewhat dominant at least in MEC. Furthermore, we observed that cisplatin induced Bmi-1 expression in parallel with pS6K1 expression in vitro and that cisplatin alone or cisplatin-first combination therapy induced both of them in vivo. In contrast, temsirolimus-first or concurrent combination therapy blocked increases in pS6K1 and Bmi-1 expression. Previous study in ovarian cancer showed that knockdown of S6K1 decreased expression of Bmi-1 and sphere formation (Ma et al. 2018). As such, it is likely that cisplatin induces Bmi-1 expression through activation of pS6K1 signaling. Notably, temsirolimus-first or concurrent combination therapy can overcome cisplatin-induced expression of pS6K1 and Bmi-1 and increase the CSC fraction more effectively than combination therapy with cisplatin first.

This work was designed to investigate the impact of therapy on CSCs. As such, we had to perform short-term in vivo experiments, and our major readout is not tumor size/volume but rather impacts on stemness. We observed significant effects of all single and combination therapies on tumor size, but due to the short duration of the treatment (10 d), we are unable to distinguish effects among different therapeutic combinations. We respectfully suggest that this should not be considered a shortcoming of this study but rather a by-product of the fact that experiments were designed for the study of impacts on CSCs. We are now developing a long-term study (1-y follow-up) testing the effect of neoadjuvant therapy with temsirolimus and cisplatin (the most promising drug combination unveiled here) on the recurrence/metastasis of MECs, as we did with an MDM2 inhibitor in models of adenoid cystic carcinoma (Nör et al. 2017).

We observed that cisplatin caused an increase in the number and size of salispheres in a dose-dependent manner and increased the fraction of CSCs in vivo. These data correlate well with known clinical shortcomings of cisplatin. While cisplatin has a cytotoxic effect on "bulk" MEC tumor cells and may cause temporary tumor regression, it does not kill the uniquely tumorigenic MEC CSCs. The resistance of CSCs may explain, at least in part, the high incidence of tumor relapse experienced by patients with MEC. In contrast, temsirolimus inhibited the generation of salispheres and expression of Bmi-1 and decreased the fraction of CSCs in vivo, while it had limited impact at disrupting existing salispheres in vitro. These data suggest that temsirolimus inhibits the formation and clonal expansion of CSCs and that this therapeutic strategy might be beneficial for treatment of malignancies that follow the cancer stem cell hypothesis.

In summary, this work provides initial preclinical evidence for a new treatment strategy for MEC that is based on the use of an mTOR inhibitor (to ablate CSCs) with platinum-based cytotoxic therapy (to debulk the tumor). We observed that it is preferable to start treatment with the mTOR inhibitor and then administer cisplatin or to start the mTOR inhibitor and the cisplatin together to maximize the impact of therapy on the survival of CSCs. Inspired by recent data from the Wang laboratory in HNSCC (Jia et al. 2020), the next steps in this project will be to assess the impact of pretreatment with an antistemness agent (e.g., small molecule inhibitor of Bmi-1) or an immune checkpoint inhibitor (e.g., anti-PD-1 antibody) with an agent targeting the mTOR signaling pathway. While this project tested well-known agents for cytotoxic "debulking" of the tumor (cisplatin) and for ablation of CSCs (temsirolimus) in an attempt to speed up clinical translation, the field of salivary gland MEC research will benefit from the development of new, mechanism-based agents that demonstrate safety and long-term efficacy in the treatment of patients with this rare malignancy.

Author Contributions

T. Nakano, contributed to conception, design, data acquisition, analysis, and interpretation, drafted and critically revised the manuscript; K.A. Warner, contributed to conception and design, critically revised the manuscript; A.E. Oklejas, Z. Zhang, C. Rodriguez-Ramirez, A.G. Shuman, contributed to data acquisition, critically revised the manuscript; J.E. Nör, contributed to conception, design, data analysis and interpretation of data, critically revised the manuscript. All authors gave final approval and agree to be accountable for all aspects of the work.

Acknowledgments

We thank the patients for kindly giving the tumor specimens used to generate the cell lines and xenograft models of mucoepidermoid

carcinoma that enabled this research project. We also thank the University of Michigan Histology and Flow Cytometry Cores for their skillful supports. We also thank Sosuke Sahara for his excellent technical support.

Declaration of Conflicting Interests

The authors declared no potential conflicts of interest with respect to the research, authorship, and/or publication of this article.

Funding

The authors disclosed receipt of the following financial support for the research, authorship, and/or publication of this article: This work was funded by grants from the Uehara Memorial Foundation and Soda Toyoji Memorial Foundation (to T.N.) and the National Institutes of Health / National Institute of Dental and Craniofacial Research (grants R01-DE021139 and R01-DE023220 to J.E.N.).

ORCID iD

J.E. Nör https://orcid.org/0000-0002-4056-0235

References

Adams A, Warner K, Pearson AT, Zhang Z, Kim HS, Mochizuki D, Basura G, Helman J, Mantesso A, Castilho RM, et al. 2015. ALDH/CD44 identifies uniquely tumorigenic cancer stem cells in salivary gland mucoepidermoid carcinomas. Oncotarget. 6(29):26633–26650.

Adams A, Warner KA, Nör JE. 2013. Salivary gland cancer stem cells. Oral Oncol. 9(9):845–853.

Ailles LE, Weissman IL. 2007. Cancer stem cells in solid tumors. Curr Opin Biotechnol. 18(5):460–466.

Alfieri S, Granata R, Bergamini C, Resteghini C, Bossi P, Licitra LF, Locati LD. 2017. Systemic therapy in metastatic salivary gland carcinomas: a pathology-driven paradigm? Oral Oncol. 66:58–63.

Al-Hajj M, Wicha MS, Benito-Hernandez A, Morrison SJ, Clarke MF. 2003. Prospective identification of tumorigenic breast cancer cells. Proc Natl Acad Sci U S A. 100(7):3983–3988.

Andrews A, Warner K, Rodriguez-Ramirez C, Pearson AT, Nör F, Zhang Z, Kerk S, Kulkarni A, Helman JI, Brenner JC, et al. 2019. Ablation of cancer stem cells by therapeutic inhibition of the MDM2-p53 interaction in mucoepidermoid carcinoma. Clin Cancer Res. 25(5):1588–1600.

Carmalt JL, Simhofer H, Bienert-Zeit A, Rawlinson JE, Waldner CL. 2009. Association of reactive oxygen species levels and radioresistance in cancer stem cells. Nature. 458(7239):780–783.

Charafe-Jauffret E, Ginestier C, Iovino F, Tarpin C, Diebel M, Esterni B, Houvenaeghel G, Extra JM, Bertucci F, Jacquemier J, et al. 2010. Aldehyde dehydrogenase 1-positive cancer stem cells mediate metastasis and poor clinical outcome in inflammatory breast cancer. Clin Cancer Res. 16(1):45–55.

Chen AM, Granchi PJ, Garcia J, Bucci MK, Fu KK, Eisele DW. 2007. Local-regional recurrence after surgery without postoperative irradiation for carcinomas of the major salivary glands: implications for adjuvant therapy. Int J Radiat Oncol Biol Phys. 67(4):982–987.

Chen J, Li Y, Yu TS, McKay RM, Burns DK, Kernie SG, Parada LF. 2012. A restricted cell population propagates glioblastoma growth after chemotherapy. Nature. 488(7412):522–526.

Chinn SB, Darr OA, Owen JH, Bellile E, McHugh JB, Spector ME, Papagerakis SM, Chepeha DB, Bradford CR, Carey TE, et al. 2015. Cancer stem cells: mediators of tumorigenesis and metastasis in head and neck squamous cell carcinoma. Head Neck. 37(3):317–326.

Fitzgerald TL, McCubrey JA. 2014. Pancreatic cancer stem cells: association with cell surface markers, prognosis, resistance, metastasis and treatment. Adv Biol Regul. 56:45–50.

Hambardzumyan D, Squatrito M, Holland EC. 2006. Radiation resistance and stem-like cells in brain tumors. Cancer Cell. 10(6):454–456.

Hu Y, Guo R, Wei J, Zhou Y, Ji W, Liu J, Zhi X, Zhang J. 2015. Effects of PI3K inhibitor NVP-BKM120 on overcoming drug resistance and eliminating cancer stem cells in human breast cancer cells. Cell Death Dis. 6(12):e2020.

Janku F, Yap TA, Meric-Bernstam F. 2018. Targeting the PI3K pathway in cancer: are we making headway? Nat Rev Clin Oncol. 15(5):273–291.

Jia L, Zhang W, Wang CY. 2020. Bmi-1 inhibition eliminates residual cancer stem cells after PD1 blockade and activates antitumor immunity to prevent metastasis and relapse. Cell Stem Cell. 27(2):238–253.e6.

Keysar SB, Le PN, Miller B, Jackson BC, Eagles JR, Nieto C, Kim J, Tang B, Glogowska MJ, Morton JJ, et al. 2016. Regulation of head and neck squamous cancer stem cells by PI3K and SOX2. J Natl Cancer Inst. 109(1):djw189.

Kim J, Shin JH, Chen CH, Cruz L, Farnebo L, Yang J, Borges P, Kang G, Mochly-Rosen D, Sunwoo JB. 2017. Targeting aldehyde dehydrogenase activity in head and neck squamous cell carcinoma with a novel small molecule inhibitor. Oncotarget. 8(32):52345–52356.

Korkaya H, Kim GI, Davis A, Malik F, Henry NL, Ithimakin S, Quraishi AA, Tawakkol N, D'Angelo R, Paulson AK, et al. 2012. Activation of an IL6 inflammatory loop mediates trastuzumab resistance in HER2+ breast cancer by expanding the cancer stem cell population. Mol Cell. 47(4):570–584.

Laurie SA, Licitra L. 2006. Systemic therapy in the palliative management of advanced salivary gland cancers. J Clin Oncol. 24(17):2673–2678.

Liu Q, Li Q, Zhu S, Yi Y, Cao Q. 2019. B lymphoma Moloney murine leukemia virus insertion region 1: an oncogenic mediator in prostate cancer. Asian J Androl. 21(3):224–232.

Luna MA. 2006. Salivary mucoepidermoid carcinoma: revisited. Adv Anat Pathol. 13(6):293–307.

Ma J, Kala S, Yung S, Chan TM, Cao Y, Jiang Y, Liu X, Giorgio S, Peng L, Wong A. 2018. Blocking stemness and metastatic properties of ovarian cancer cells by targeting p70S6K with dendrimer nanovector-based siRNA delivery. Mol Ther. 26(1):70–83.

Magaway C, Kim E, Jacinto E. 2019. Targeting mTOR and metabolism in cancer: lessons and innovations. Cells. 8(12):1584.

Nacerddine K, Beaudry JB, Ginjala V, Westerman B, Mattiroli F, Song JY, van der Poel H, Ponz OB, Pritchard C, Cornelissen-Steijger P, et al. 2012. Akt-mediated phosphorylation of Bmi1 modulates its oncogenic potential, E3 ligase activity, and DNA damage repair activity in mouse prostate cancer. J Clin Invest. 122(5):1920–1932.

Nör C, Zhang Z, Warner KA, Bernardi L, Visioli F, Helman JI, Roesler R, Nör JE. 2014. Cisplatin induces Bmi-1 and enhances the stem cell fraction in head and neck cancer. Neoplasia. 16(2):137–146.

Nör F, Warner KA, Zhang Z, Acasigua G, Pearson AT, Kerk S, Helman JI, Sant'Ana Filho M, Wang S, Nör JE. 2017. Therapeutic inhibition of the MDM2-p53 interaction prevents recurrence of adenoid cystic carcinomas. Clin Cancer Res. 23(4):1036–1048.

Ocana A, Vera-Badillo F, Al-Mubarak M, Templeton AJ, Corrales-Sanchez V, Diez-Gonzalez L, Cuenca-Lopez MD, Seruga B, Pandiella A, Amir E. 2014. Activation of the PI3K/mTOR/AKT pathway and survival in solid tumors: systematic review and meta-analysis. PLoS One. 9(4):e95219.

Saxton RA, Sabatini DM. 2017. mTOR signaling in growth, metabolism, and disease. Cell. 169(2):361–371.

Trucco MM, Meyer CF, Thornton KA, Shah P, Chen AR, Wilky BA, Carrera-Haro MA, Boyer LC, Ferreira MF, Shafique U, et al. 2018. A phase II study of temsirolimus and liposomal doxorubicin for patients with recurrent and refractory bone and soft tissue sarcomas. Clin Sarcoma Res. 8:21.

Vander Poorten V, Hunt J, Bradley PJ, Haigentz M Jr, Rinaldo A, Mendenhall WM, Suarez C, Silver C, Takes RP, Ferlito A. 2014. Recent trends in the management of minor salivary gland carcinoma. Head Neck. 36(3):444–455.

Vergadi E, Ieronymaki E, Lyroni K, Vaporidi K, Tsatsanis C. 2017. Akt signaling pathway in macrophage activation and M1/M2 polarization. J Immunol. 198(3):1006–1014.

Zhang Z, Filho MS, Nör JE. 2012. The biology of head and neck cancer stem cells. Oral Oncol. 48(1):1–9.

Zhou H, Yu C, Kong L, Xu X, Yan J, Li Y, An T, Gong L, Gong Y, Zhu H, et al. 2019. B591, a novel specific pan-PI3K inhibitor, preferentially targets cancer stem cells. Oncogene. 38(18):3371–3386.